ELSEVIER

Materials Science and Engineering A345 (2003) 172–178

MATERIALS SCIENCE & ENGINEERING A

www.elsevier.com/locate/msea

Simulation of stresses and delamination in a plasma-sprayed thermal barrier system upon thermal cycling

M.Y. He [a,*], J.W. Hutchinson [b], A.G. Evans [a]

[a] *Materials Department, University of California, Santa Barbara, CA 93106 5050, USA*
[b] *Division of Engineering and Applied Science, Harvard University, Cambridge, MA 02138, USA*

Received 21 February 2002; received in revised form 14 June 2002

Abstract

A thermal barrier system with plasma-sprayed thermal barrier coating (TBC) has been analyzed subject to thermal cycling. The thermally grown oxide (TGO) is allowed to grow at the peak temperature in the cycle, with both thickening and lateral components of the growth strain. The stresses in the TGO are also allowed to relax at high temperature when they attain a critical level. The bond coat is allowed to yield with temperature dependent yield strength. The stresses induced in the TBC and in the TGO have been calculated. The vertical component of the stress in the TBC is shown to have a large tensile domain with a maximum that increases systematically as the system cycles. There is a corresponding increase in the amplitude of the interface undulations. The stresses in the TBC have been used to calculate energy release rates, G, for cracks in the TBC extending parallel to the interface, just above the peaks of the undulations. This analysis reveals a minimum value, G_{min} preceding instability. Equating this minimum to the TBC toughness identifies a delamination criticality.

Keywords: Plasma spray coatings; Thermal barrier systems; Computer simulation; Layered materials; Fatigue

1. Introduction

Thermal barrier systems made using plasma spray coatings are widely used in power turbines as well as on some components in aero-turbines [1–9]. The systems consist of a bond coat that provides the oxidation resistance, a thermal barrier coating (TBC) that imparts the thermal insulation and a thermally-grown oxide (TGO), primarily of α-alumina, that thickens as the system cycles. The associated morphology is depicted on Fig. 1. The oscillatory nature of the bond coat surface is deliberately created by grit blasting, before depositing the thermal barrier material. This contrasts with the preference for bond coat planarity when the coatings are made by electron-beam physical vapor deposition (EB-PVD) [8–12]. The difference is attributed to the nature of the oxide layer that forms on the bond coat as the TBC deposits.

Various investigations have probed the failure mechanisms and attempted to calculate the stresses [13–17]. The generally agreed-upon finding is that the failure occurs by delamination, proceeding along a trajectory primarily within the TBC, just above the TGO [1–6]. Locally, near the peaks of the oscillations, the delamination may penetrate the TGO and extend along the TGO/bond coat interface [13]. The details have been elusive, because of the difficulties in making sequential observations of events occurring near the interface and because all phenomena affecting the stress have yet to be included in a simulation scheme. These phenomena include the growth of the TGO, the thermal expansion misfit on cooling, visco-plasticity occurring in the bond coat and the TGO, as well as the deformation of the TBC [18–22]. In order to address this deficiency, a full numerical simulation scheme is introduced in this article. The scheme is an adaptation of a procedure developed for EB-PVD systems, previously used to simulate TGO displacement instabilities [18–22]. Prototypical stress distributions are calculated. Energy release rates are determined for expected crack ensembles, as a

* Corresponding author. Tel.: +1-805-893-7166; fax: +1-805-893-8971
E-mail address: ming@engineering.ucsb.edu (M.Y. He).

0921-5093/02/$ - see front matter
PII: S0921-5093(02)00458-6

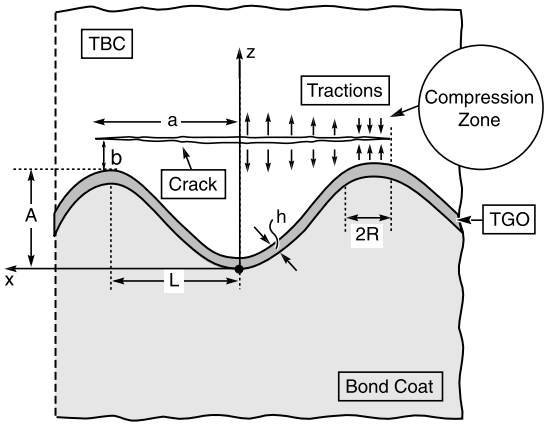

Fig. 1. A schematic of the sinusoidal configuration used for the analysis indicating the location of the cracks in the TBC and the zones of residual tension/compression induced by TGO growth and thermal cycling.

basis for establishing a delamination criterion in terms of the properties of the constituent materials.

Previous analysis [23] attempted to encapsulate the major effects brought about by the interplay between the growth and thermal expansion misfit strains. This was done within a spherical geometry intended to represent displacements and stresses expected near the apex and base of the interface oscillations, respectively. However, the analysis was restricted to TGO growth normal to the interface. In practice, some of the new TGO forms on the internal grain boundaries, resulting in a lateral growth strain [4]. For this restricted case, the stress patterns near the apex have the following principal features (Fig. 1).

i) During isothermal growth of the TGO, tensile stresses normal to the substrate are induced in the TBC between neighboring apices. This happens because of the displacement incompatibility upon TGO thickening along curved segments of the interface. These stresses may be capable of initiating cracks in the TBC. The TGO experiences in-plane tension, with compression normal to the interface. The tension may be alleviated by visco-plastic deformation of the TGO, preventing it from cracking.
ii) As the system cools and experiences the effects of thermal expansion misfit, the stress patterns change. The in-plane tension in the TGO diminishes and eventually becomes compressive. The tension normal to the TBC/TGO interface in the TBC is retained and may become larger. The compression normal to the TGO/bond coat interface may reduce.

The results of the full numerical simulations are compared and contrasted with these analytic findings.

2. Simulation scheme

The system comprises a bond coat with sinusoidal oscillations, amplitude A and wavelength, $2L$, varying as: $z=(A/2)\cos(\pi x/L)$, with $A/L=1.0$, and $h/L=0.1$ (h is the thickness of the TGO) (Fig. 1). The calculations are performed subject to generalized plane strain. The TBC is considered elastic and anisotropic, with in-plane Young's modulus, $E_{tbc}=20-100$ GPa. The bond coat has temperature-dependent yield strength of the type shown on Fig. 2(b). The strength up to temperature T_1 (300 °C in all calculations) is 1 GPa. At temperatures above T_2, the strength σ^{bc}_{Ymin} is typically 100 MPa. It changes linearly from $T_1 \rightarrow T_2$. The bond coat is assigned a thermal expansion misfit with the superalloy substrate. For most calculations it is: $\Delta\alpha \equiv \alpha_{sub}-\alpha_{bc}=+3$ ppm per °C [24].

Stress redistribution in the TGO is simulated by imparting the yield characteristics plotted on Fig. 2(a) [19]. That is, at the peak temperature, the TGO yields when the Mises stress reaches ± 1 GPa, imposing a maximum on the growth stress [9,19]. On cooling and reheating it behaves elastically, because of the rapid increase in yield strength at lower temperatures. The misfit stress at ambient equals the sum of that from growth with that from thermal expansion misfit ($\sigma_{ambient} \approx -4.5$ GPa) [8,25–27].

From experiences with EB-PVD systems, these properties appear to capture the principal non-linearities, as well as their effect on stresses and displacements [18–22]. The time dependence associated with creep in the

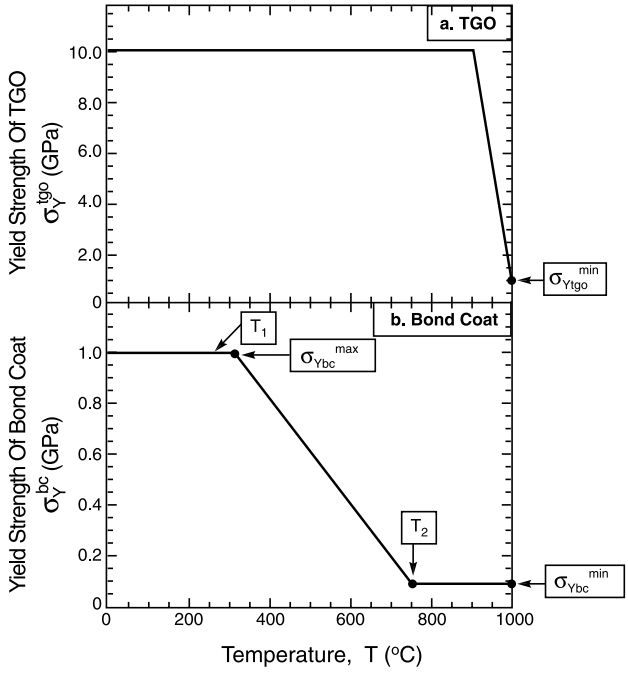

Fig. 2. Yield strength characteristics assumed for (a) the TGO and (b) the bond coat: as used in prior simulations [2,7,8].

bond coat and in the TGO appears to have little effect on the general trends, but it does introduce a cooling rate effect, that will be missed in the following simulations.

The temperature is cycled over a range, $\Delta T = 1000\ ^\circ C$, and the stresses, as well as the plastic strains, and the oscillation amplitudes are monitored. The TGO is allowed to grow at the peak temperature in the cycle, with both thickening and lateral components of the growth strain. The lateral component, $\Delta\varepsilon_{xx} = \Delta\varepsilon_{zz} = \varepsilon_g$ (ε_g is taken to be 0.001 in the following calculations) is incorporated by imposing a transformation strain to all elements in the TGO layer, taken to be uniform through the thickness. For the thickening simulation a strain ε_t is imposed on the row of the bond coat elements immediately adjacent to the TGO. Simultaneously, the properties of these elements are switched from those characteristic of the bond coat to those applicable to the TGO. The chosen thickening rate dictates the dimensions of the elements that undergo oxidation. For simplicity, most of the calculations are performed for linear TGO growth kinetics with $\Delta h/2L = 0.005$ or 0.01 [18,19]. In a few cases, parabolic growth conditions are used [9,21].

The other elastic material properties are the same as those used in the previous analyses [18,19] ($E_{sub} = 200$ GPa, $\nu_{sub} = 0.3$, $\alpha_{sub} = 18$ ppm per $^\circ C$, $E_{bc} = 200$ GPa, $\nu_{bc} = 0.3$, $\alpha_{bc} = 15$ ppm per $^\circ C$, $E_{tgo} = 400$ GPa, $\nu_{tgo} = 0.2$, $\alpha_{tgo} = 8$ ppm per $^\circ C$, and $\alpha_{TBC} = 11$ ppm per $^\circ C$).

3. Stresses

3.1. Stresses in the TBC

The stresses having greatest relevance to delamination are those normal to the interface, σ_{zz}^{tbc}: they prescribe the delamination energy release rate. The stresses are normalized by the misfit stress [23], $\sigma_o^* = E_{tbc}\Delta\alpha_{tbc}\Delta T/(1-\nu_{tbc})$. A typical result for σ_{zz}^{tbc} (Figs. 3 and 4), indicates features relevant to TBC cracking. At ambient, in a small region around the apex, the stress is compressive. Elsewhere, the TBC experiences a relatively uniform tension. The stresses increase as the system cycles, because of the displacements caused by the thickening of the TGO. Within a single cycle, the magnitude is almost the same at both ambient and elevated temperature. The peak tension just beyond the apex (Fig. 4) increases in a nominally linear manner with the number of cycles, N (Fig. 5):

$$\sigma_{zz}^{max} = \sigma_i + N\Delta\sigma_N \quad (1)$$

The stresses σ_i and $\Delta\sigma_N$ are summarized on Table 1. This increase in stress with N is a prerequisite for cyclic cracking in the TBC. None of the previous attempts at simulation has demonstrated this systematic stress increase in the TBC.

Some of the material properties that affect the increase in tensile stress are evident from Fig. 5, Table 1. Namely, higher stresses arise as the modulus of the TBC and the high temperature yield strength for the bond coat increase. The latter happens because the plastic deformation occurring in the bond coat redistributes and alleviates the highest stresses in the TBC.

3.2. Stresses in the TGO

At ambient, the stresses in the TGO are compressive at all locations (Fig. 6(a and b)). Moreover, the stress changes that occur upon cycling are quite small. Note that the stresses are much lower than the thermal expansion misfit stress [9,23], $\sigma_o = E_{tgo}\Delta\alpha_{tgo}\Delta T/(1-\nu_{tgo})$. In a typical case, $\sigma_{xx}^{tgo} \approx 0.2$ whereas for planar interfaces, $\sigma_{xx}^{tgo} \to \sigma_0$ [18,21,23]. These relatively low values are associated with the alleviation in stress caused by plastic deformation in the bond coat.

Distributions of the stresses determined at the temperature maximum (Fig. 7) reveal zones of both tension and compression. The zone subject to tension determines whether the TGO becomes susceptible to cracking as the system cycles. When the bond coat has temperature invariant yield strength ($\sigma_Y^{bc} = 400$ MPa), on average, σ_{xx}^{tgo} and σ_{zz}^{tgo} are predominantly tensile after cycling, with a small region of compression near the apex. The compression exists because of the lateral component of the growth strain. That is, thickening without lateral growth causes σ_{xx}^{tgo} tension at the apex [23]. When yielding is temperature dependent ($\sigma_{Ymin}^{bc} = 100$ MPa), both stress components (Fig. 8) become predominantly compressive after about ten cycles.

The use of a parabolic growth law for the TGO [21] does not affect the trends. The only slight difference is a larger zone subject to tension (Fig. 7).

4. Strains and displacements

The plastic strains that accumulate in the bond coat are typical of those discussed previously [18–22]. Namely, for the property choices used in these simulations, the bond coat yields on cooling, resulting in plastic strains and non-linear interface displacements. It also re-yields on heating, such that additional plastic strains occur. The corresponding changes in the oscillation amplitude, ΔA, upon cycling (Fig. 9) indicate behaviors similar to those discussed elsewhere [18–22]. Under the chosen conditions, the amplitude gradually increases with cycling. The rate, $d\Delta A/dN$, becomes slightly larger as the thickening per cycle increases. The relevance to the present problem is that the change in amplitude stretches the adjacent TBC in the z-

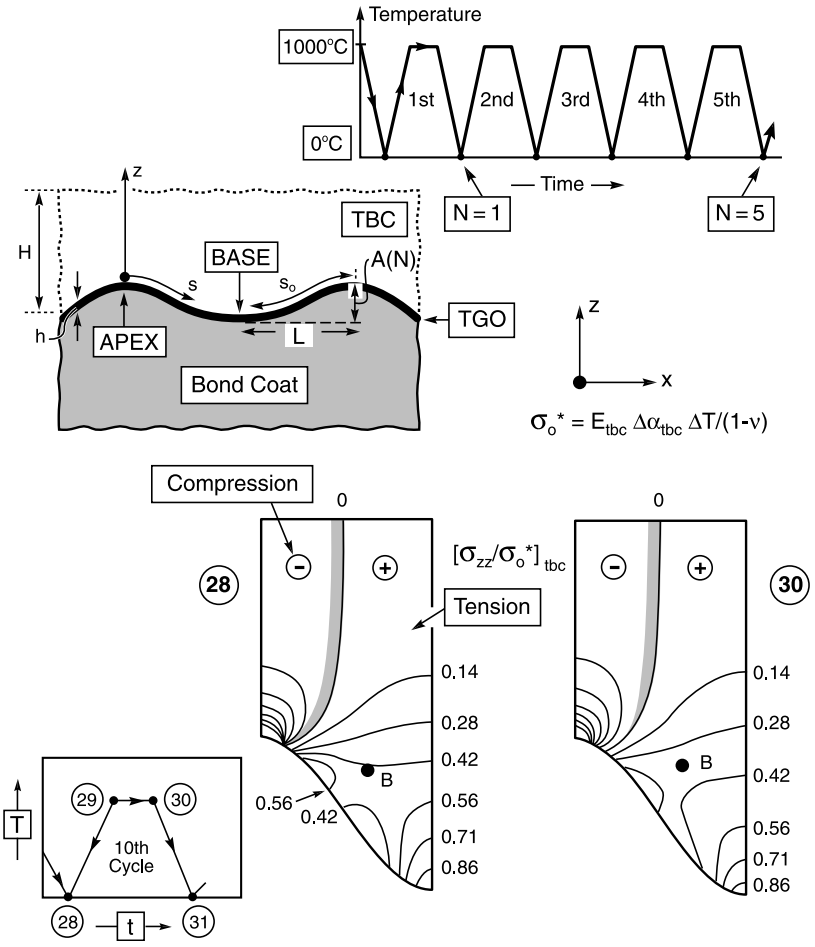

Fig. 3. The zones of σ_{zz} tension and compression induced in the TBC at two stages of the tenth cycle (#28 and 30), indicated on the lower left insert. The coordinates and the cycling conditions are shown, as well as the geometry. Note that the stresses are insensitive to the stage chosen in that cycle. ($E_{tbc} = 40$ GPa, $\sigma^{bc}_{Ymin} = 100$ MPa, $\Delta h/2L = 0.01$).

direction. This stretching is the source of the systematic increase in σ^{tbc}_{zz} with N, revealed on Fig. 5, Eq. (1). Note that changes in the bond coat strength that occur during exposure, as the Al content reduces, affect the stresses in the TBC, in the sense that a softening trend increases the TGO displacement and increases the stresses [19].

5. Energy release rates

In order to simulate cracking and delamination of the TBC, a crack pattern must be chosen, the energy release rate, G, determined and compared with the fracture toughness, Γ_{tbc}, of the YSZ. One possibility would be to place a periodic array of cracks in the TBC within the zone of σ^{tbc}_{zz} tension and calculate G as the cracks extend. However, when such an array converges, mode I G necessarily reduces to zero [28].

Yet, experimental observations reveal that a material with a random dispersion of residually compressed spheres can spontaneously crack [29]. This happens in the following manner. A crack that initiates in the tensile field of the matrix arrests at the compressed particles it first encounters. Once the crack penetrates through these particles, it becomes unstable and extends throughout the material. This condition is satisfied once the quantity, $\zeta \equiv \sigma_o\sqrt{R}$, exceeds a critical value (where R is the sphere radius, σ_o the residual stress in the particle). The analogous problem within the present context is that depicted on Fig. 1. Namely, once a crack that forms within the tensile zone is able to penetrate through the compression zone at the apex, it becomes unstable and delaminates the TBC.

The crack exhibits the energy release rate characteristics depicted on Fig. 10(a). The initial increase from zero varies as $G \sim \sqrt{a}$, comparable to a small crack subject to uniform tension. When the crack reaches the compressed particles, G exhibits a peak, it then decreases as it penetrates the compression zone. Once it extends through the particles, and re-enters the tensile field, G increases again. The consequence is a minimum, G_{min}. The crack system becomes unstable subject to the criterion, $G_{min} \geq \Gamma_{tbc}$ since thereafter, G exceeds the toughness.

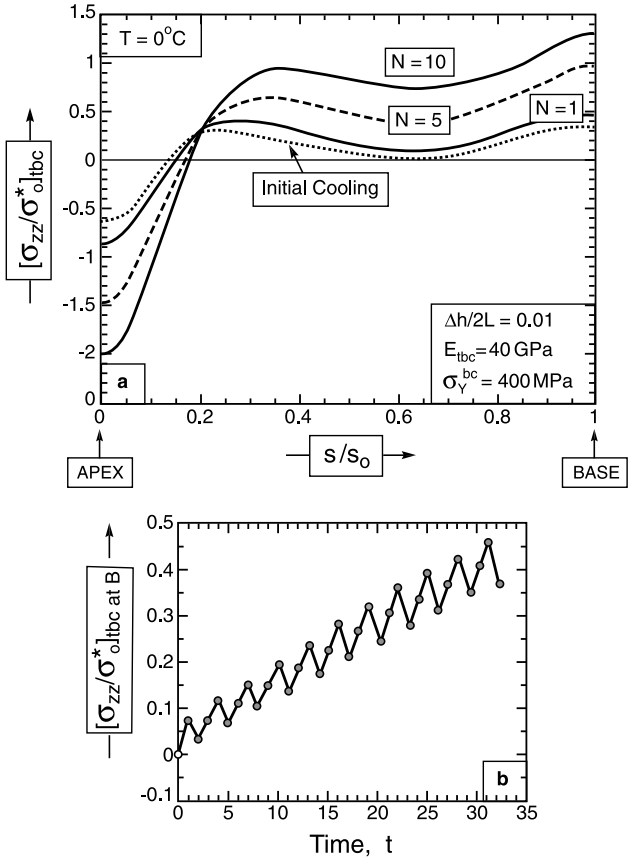

Fig. 4. Some specific variations of the σ_{zz} stress in the TBC. (a) The distribution of stress along the interface with the TGO at ambient temperature for cycles 1, 5 and 10. (b) The change in stress at a single location B (refer to Fig. 3) as the temperature cycles. ($E_{tbc} = 40$ GPa, $\sigma_Y^{bc} = 400$ MPa, $\Delta h/2L = 0.01$).

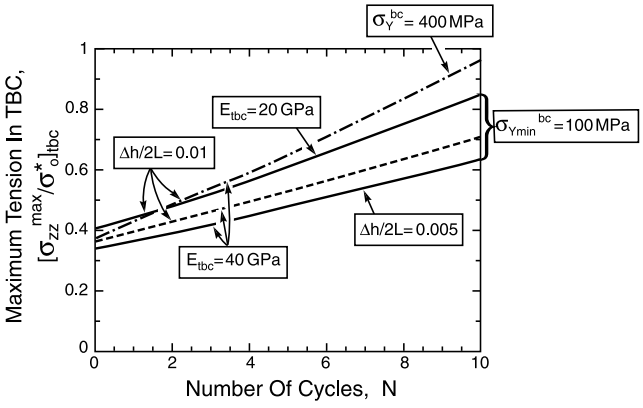

Fig. 5. Changes in the maximum σ_{zz} tension in the TBC upon cycling for several choices of the TBC modulus, E_{tbc}, the TGO growth rate, $\Delta h/2L$, and the bond coat mechanical properties.

Finite element results for energy release rate have been obtained for the plane strain crack shown in Fig. 1. Cell model calculations performed subject to thermal cycling and TGO growth affirm the features shown on Fig. 10(a). Detailed calculations in the vicinity of the minimum, determined for a crack close to the undulation peak, $b/2L = 0.02$, give the result plotted on Fig. 10(b). Namely, beyond about ten cycles, G_{min} increases almost linearly with further cycling. Non-dimensional analysis indicates that the result can be expressed in the form:

$$\frac{G_{min}}{E_{tbc}L(\Delta\alpha\Delta T)^2} = \kappa(N - N_o) \quad (2)$$

with $N_o \approx 8$ and $\kappa \approx 9 \times 10^{-3}$. The relationship (2) can be used as a failure criterion, elaborated below. The fundamental basis for this trend is addressed separately [30]. The occurrence of the minimum, G_{min}, its dependence on the morphological details, and the precise evolution of the crack as it extends between the zones of compression represent a class of fundamental unsolved

Table 1
Values of σ_i and $\Delta\sigma_N$

Bond coat yield strength (MPa)	E_{tbc} (GPa)	$\Delta h/2L$	σ_i/σ_o^*	$\Delta\sigma_N/\sigma_o^*$
$\sigma_{Ymin}^{bc} = 100$	40	0.01	0.36	0.036
$\sigma_{Ymin}^{bc} = 100$	20	0.01	0.39	0.047
$\sigma_{Ymin}^{bc} = 100$	40	0.005	0.33	0.031
$\sigma_Y^{bc} = 400$	40	0.01	0.33	0.065

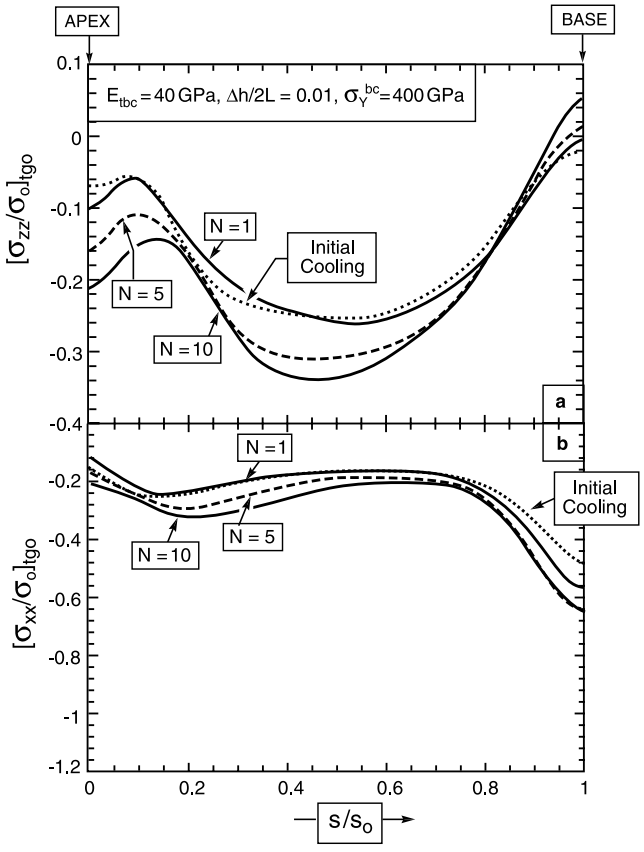

Fig. 6. The normal, σ_{zz} and in-plane, σ_{xx} stresses in the TGO at ambient adjacent to the interface with the bond coat after 1, 5 and 10 cycles. ($E_{tbc} = 40$ GPa, $\sigma_Y^{bc} = 400$ MPa, $\Delta h/2L = 0.01$).

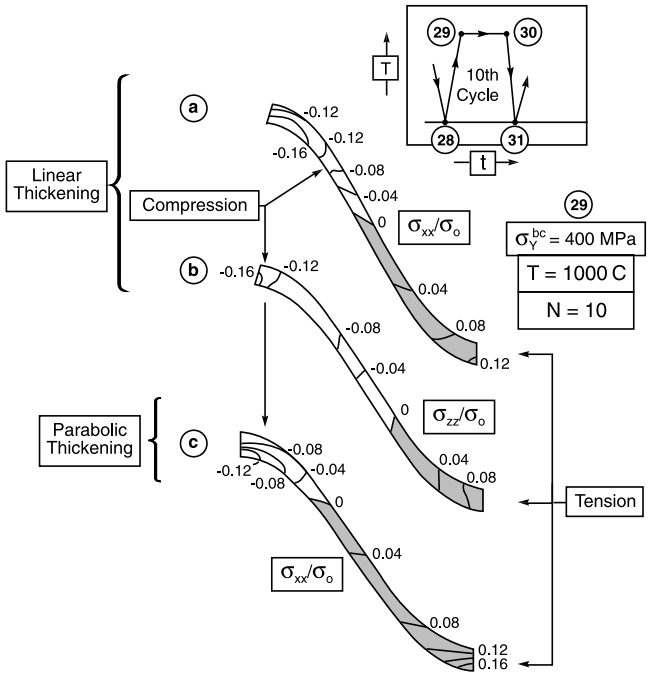

Fig. 7. The zones of tension and compression in the TGO at the temperature maximum. ($E_{tbc} = 40$ GPa, $\sigma_Y^{bc} = 400$ MPa, $\Delta h/2L = 0.01$).

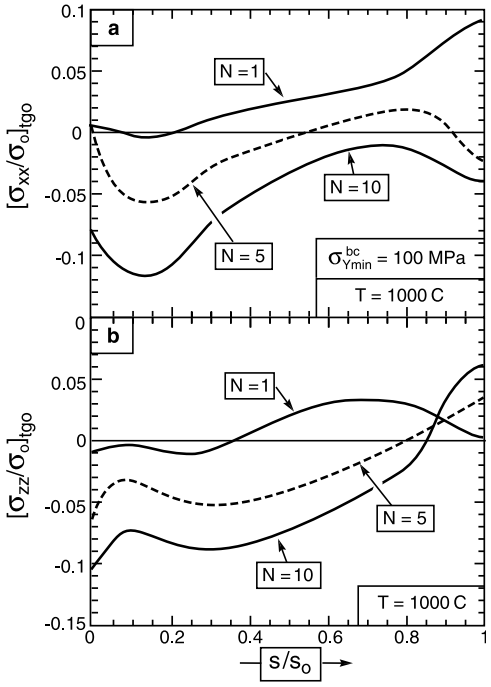

Fig. 8. The stresses in the TGO corresponding to Fig. 6 at the temperature maximum. ($E_{tbc} = 40$ GPa, $\sigma_{Ymin}^{bc} = 100$ MPa, $\Delta h/2L = 0.01$).

problems in fracture mechanics. These fundamentals are addressed in a separate investigation [30].

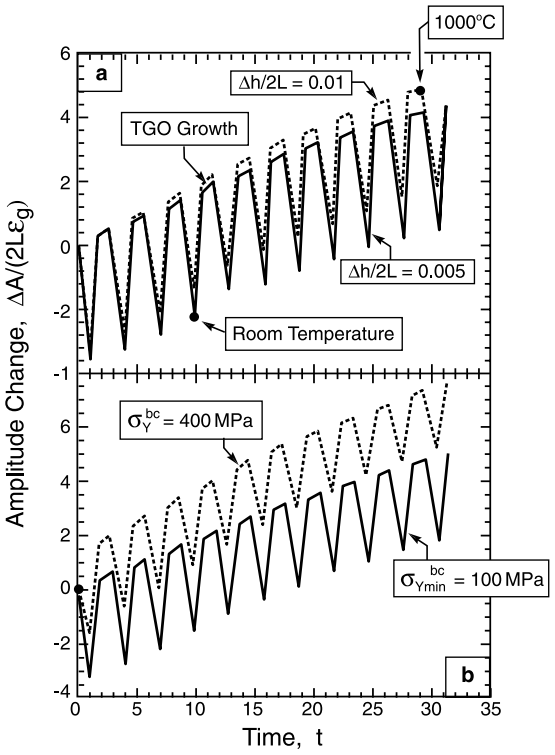

Fig. 9. Changes in the amplitude of the interface oscillations as the system thermally cycles. (a) Comparison for different TGO thickening rates, $\Delta h/2L = 0.005$ and 0.01 for, $\sigma_{Ymin}^{bc} = 100$ MPa. (b) Comparison for different bond coat yield strengths, $\sigma_Y^{bc} = 400$ MPa and $\sigma_{Ymin}^{bc} = 100$ MPa for $\Delta h/2L = 0.01$.

6. Failure criterion

Once the energy release rate minimum, G_{min}, reaches the TBC fracture toughness (at the appropriate mode mixity), Γ_{tbc}, a crack originating in the tensile zone between the peaks becomes unstable and extends into a delamination crack. Equating G_{min} in (Eq. (2)) to the toughness provides an expression for the number of cycles to failure,

$$N_f = N_o + \frac{\Gamma_{tbc}}{E_{tbc} L (\Delta\alpha \Delta T)^2 \kappa} \tag{3}$$

This expression is considered prototypical rather than specific, in the sense that κ is dependent on the assumptions made about the TGO growth strain, as well as its yield strength and on the mechanical properties of the bond coat. To assess whether (Eq. (3)) yields reasonable magnitudes, inserting typical choices ($E_{tbc} =$ 40 GPa, $\Gamma_{tbc} = 50$ J m^{-2}, $\Delta\alpha = 4$ ppm per °C) reveals that, for the TGO and bond coat characteristics chosen for the present calculations, N_f, is of order 400 cycles. However, we emphasize that the result should only be compared with experiment once the constituent properties have been ascertained with some precision.

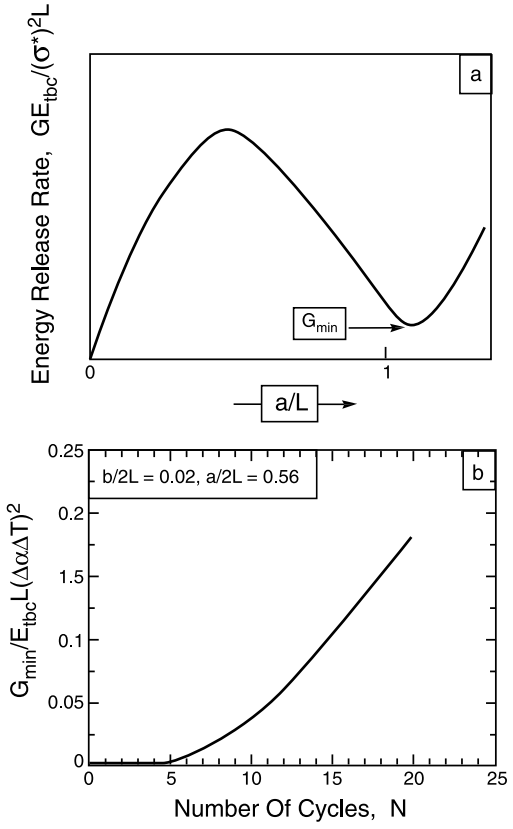

Fig. 10. (a) A schematic of the energy release rate as a function of crack length. (b) Changes in the minimum energy release rate upon cycling.

7. Conclusion

It has been shown that TGO growth, inclusive of a lateral strain, in conjunction with the thermal expansion misfit upon thermal cycling, induces tensile stresses in the TBC normal to the surface. These stresses increase in a nominally linear manner with the number of cycles, N. They increase because small changes in the amplitude of the interfacial oscillations stretch the adjacent TBC normal to the surface. These amplitude changes are mechanistically related to the displacement instabilities found in systems with EB-PVD coatings on Pt–aluminide bond coats.

The changes in stress with cycling have been related to an increase in the energy release rate for cracks that originate within the tensile zone between peaks in the interface oscillations. These cracks penetrate through the islands of compression above the peaks, subject to a minimum in the energy release rate, $G_{\min}$. Abrupt failure occurs when $G_{\min}$ exceeds the fracture toughness of the TBC.

A criterion for delamination has been derived upon relating the number of cycles at which $G_{\min} \rightarrow \Gamma_{tbc}$ to the TBC modulus and the dimensions of the interface oscillations.

References

[1] R.A. Miller, J. Am. Ceram. Soc. 67 (1984) 517.
[2] J.T. DeMasi-Marcin, D.K. Gupta, Surf. Coatings Technol. 68/69 (1994) 1–9.
[3] NRC Report, R. Hillery (Ed.), Coatings For High Temperature Structural Materials, National Academy Press, 1996.
[4] S.M. Meier, D.K. Gupta, Trans. ASME 116 (1993) 250–257.
[5] T.A. Cruse, S.E. Stewart, M. Ortiz, J. Eng. Gas Turbines Power 110 (1988) 610.
[6] J.T. DeMasi-Marcin, K.D. Sheffler, S. Bose, ASME Paper 89-GT-132, American Society of Mechanical Engineering, New York, 1989.
[7] E.Y. Lee, R.D. Sisson, in: C.C. Berndt, S. Sampath (Eds.), Proceedings of Seventh National Thermal Spray Conference, ASM International, Materials Park, OH, 1994, pp. 55–59.
[8] M.J. Stiger, N.M. Yanar, M.G. Topping, F.S. Pettit, G.H. Meier, Z. Metallk 90 (1999) 1069–1078.
[9] A.G. Evans, D.R. Mumm, J.W. Hutchinson, G.H. Meier, F.S. Pettit, Prog. Mater. Sci. 46 (2001) 505–553.
[10] P.K. Wright, A.G. Evans, Curr. Opin. Solid State Mater. Sci. 4 (1999) 255–265.
[11] P.K. Wright, Mat. Sci. Eng. A245 (1998) 191–200.
[12] D.V. Rigney, R. Viguie, D.J. Wortman, W.W. Skelly, Proceedings of the Workshop on Thermal Barrier Coatings, NASA-CP-3312, NASA Lewis Research Center, 1995, pp. 135–150.
[13] A. Rabiei, A.G. Evans, Acta Mater. 48 (2000) 3963–3976.
[14] E.P. Busso, J. Lin, S. Sakurai, Nakayama, Acta Mater. 49 (2001) 1515–1528.
[15] E.P. Busso, J. Lin, S. Sakurai, Acta Mater. 49 (2001) 1529–1536.
[16] R. Vaßen, G. Kerkhoff, D. Stover, Mater. Sci. Eng. A303 (2001) 100–109.
[17] E. Tzimas, H. Mullejans, S.D. Peteves, J. Bressers, W. Stamm, Acta Mater. 48 (2000) 4699–4707.
[18] M.Y. He, A.G. Evans, J.W. Hutchinson, Acta Mater. 48 (2000) 2593–2601.
[19] A.M. Karlsson, A.G. Evans, Acta Mater. 49 (2001) 1793–1804.
[20] J.M. Ambrico, M.R. Begley, E.H. Jordan, Acta Mater. 49 (2001) 1577–1588.
[21] M.Y. He, J.W. Hutchinson, A.G. Evans, Acta Mater. 50 (2002) 1063–1073.
[22] A.M. Karlsson, A.G. Evans, J.W. Hutchinson, J. Mech. Phys. Solids 50 (2002) 1793–1804.
[23] A.G. Evans, M.Y. He, J.W. Hutchinson, Prog. Mater. Sci. 46 (2001) 249–271.
[24] M. Watanabe, D.R. Mumm, S. Chiras, A.G. Evans, Scr. Mater. 46 (2002) 67–70.
[25] D.M. Lipkin, D.R. Clarke, Oxid. Met. 45 (1996) 267–280.
[26] V.K. Tolpygo, D.R. Clarke, Oxid. Met. 49 (1998) 187–211.
[27] V.K. Tolpygo, D.R. Clarke, Acta Mater. 46 (1998) 5153–5166.
[28] M.Y. He, A.G. Evans, J.W. Hutchinson, Acta Mater. 45 (1997) 3481–3489.
[29] R.W. Davidge, T. Green, J. Mater. Sci. 3 (1968) 619–634.
[30] X. Chen, M.Y. He, A.G. Evans, J.W. Hutchinson, to be published.